Anal Bioanal Chem (2010) 397:3553–3561
DOI 10.1007/s00216-010-3868-4

ORIGINAL PAPER

Label-free amperometric immunobiosensor based on a gold colloid and Prussian blue nanocomposite film modified carbon ionic liquid electrode

Ke-Jing Huang · De-Jun Niu · Jun-Yong Sun · Xiao-Li Zhu · Jun-Jie Zhu

Received: 15 April 2010 / Revised: 10 May 2010 / Accepted: 20 May 2010 / Published online: 25 June 2010

Abstract A novel experimental methodology based on a Prussian blue (PB) and gold nanoparticles (AuNPs) modified carbon ionic liquid electrode (CILE) was developed for use in a label-free amperometric immunosensor for the sensitive detection of human immunoglobulin G (HIgG) as a model protein. The CILE was fabricated by using the ionic liquid 1-octyl-3-methylimidazolium hexafluorophosphate as binder. Controllable electrodeposition of PB on the surface of the CILE and coating with 3-aminopropyl triethylene silane (APS) formed a film with high electronic catalytic activity and large surface area for the assembly of AuNPs and further immobilization of HIgG antibody. The electrochemistry of the formed nanocomposite biofilm was investigated by electrochemical techniques including cyclic voltammetry, differential pulse voltammetry, and electrochemical impedance spectroscopy. The HIgG concentration was measured through the decrease of amperometric responses in the corresponding specific binding of antigen and antibody. The decreased differential pulse voltammetric values were proportional to the HIgG concentration in two ranges, 0.05–1.25 ng mL^{-1} and 1.25–40 ng mL^{-1}, with a detection limit of 0.001 ng mL^{-1} (S/N=3). This electrochemical immunoassay combined the specificity of the immunological reaction with the sensitivity of the AuNPs, ionic liquid, and PB amplified electrochemical detection and would therefore be valuable for clinical immunoassays.

Keywords Amperometric immunosensor · Prussian blue · Au nanoparticles · Human immunoglobulin G · Carbon ionic liquid electrode

Electronic supplementary material The online version of this article (doi:10.1007/s00216-010-3868-4) contains supplementary material, which is available to authorized users.

K.-J. Huang · J.-J. Zhu (✉)
Key Laboratory of Analytical Chemistry for Life Science (Ministry of Education of China), School of Chemistry and Chemical Engineering, Nanjing University, Nanjing 210093, People's Republic of China
e-mail: jjzhu@nju.edu.cn

K.-J. Huang · D.-J. Niu · J.-Y. Sun · X.-L. Zhu
College of Chemistry and Chemical Engineering, Xinyang Normal University, Xinyang 464000, People's Republic of China

Introduction

Recently, there has been growing interest in developing simple, sensitive, and specific methods for environmental monitoring, food analysis, and early diagnosis of diseases in modern medicine [1–3]. Immunoassay techniques based on highly specific molecular recognition of antigens by antibodies have become the main analytical methods for such applications. Various immunoassay protocols, e.g., surface plasmon resonance, quartz crystal microbalance, chemiluminescence, and electrochemical methods, have attracted attention with the expectation of obtaining quick and sensitive immunological responses [4–7]. Among these methods, electrochemistry has been a promising alternative to conventional immunoassay techniques due to its cost efficiency, excellent sensitivity, and inexpensive instrumentation [8, 9]. Amperometric immunosensors based on enzyme-labeled antibodies or antigens are especially promising due to their relatively low detection limit and high sensitivity in various electrochemical transducer techniques. However, the labeling process of this technique is time-consuming, costly, and often leads to the denaturation of the modified biomolecules. Furthermore, the addition of a mediator such as ferrocene and its derivatives [10, 11], dyes [12], and hydroquinone [13] in the analyte solution makes

the immunoassay system complicated and increases the analysis time. Thus, it would be preferable to immobilize an appropriate mediator on the electrode surfaces to construct amperometric immunosensors [14].

Among the numerous redox-active compounds available, Prussian blue (PB) is particularly useful for biosensor applications owing to its good electrochemical properties, which can accelerate electron transfer between electrodes and enzymes [15]. PB has been applied in many areas, including electrocatalysis [16], sensors and biosensors [17, 18], and materials science [19]. Electropolymerization is extensively applied in the enzyme immobilization and biosensor design. PB can be deposited onto the electrode through an optimized electropolymerization technique and applied as a mediator for biosensors [20]. The main disadvantage reported is the lower electrochemical stability of the PB film and the subsequently lower operational stability of the PB-based biosensors at near-neutral solution pH [21] due to formation of PB that is believed to be more soluble [22]. Thus, great efforts have been made to avoid leaching of PB from the electrode surface in order to develop new sensors with high sensitivity and stability.

In the present work, 3-aminopropyl triethylene silane (APS) was coated on the surface of the electrodeposited PB film to form a stable film which prevents the leakage of redox mediators from the matrix to enhance the stability and sensitivity of the immunosensor. Moreover, this APS/PB organic-inorganic composite film can adsorb gold nanoparticles (AuNPs) through abundant amino groups of the APS. AuNPs are a well-known kind of bionanomaterial because of their large specific surface area, strong adsorption ability, good suitability, and good conductivity [23, 24]. AuNPs can strongly interact with biomaterials and have been utilized as an intermediator to immobilize antibody whilst efficiently retaining its activity and to enhance current response in the construction of a sensitive amperometric immunosensor. Therefore, AuNPs have been widely used in constructing electrical sensors such as DNA-AuNPs assemblies [25], enzymes biosensors [26], and immunosensors [27]. In this work, we selected HIgG as a model system to be immobilized on the AuNPs interface to complete this immunosensor design.

In order to further improve the sensitivity of the immunosensor, carbon ionic liquid electrode (CILE) was applied in this work. Carbon paste electrode is a type of composite electrode, which is made up of carbon particles and organic liquid. It has the advantages of the diversity of paste modification and the convenience in manipulation, providing a reliable and universal method for immobilization of active species, and has been widely applied by the electroanalytical community due to its low cost, ease of fabrication, high sensitivity for detection, and renewable surface [28, 29]. In recent years, room temperature ionic liquids (RTILs) have been increasingly explored as a new kind of modifier in the fabrication of an ionic liquid modified carbon paste electrode. RTILs can provide a remarkable increase in the electron-transfer rate of different organic and/or inorganic electroactive compounds, offer a marked decrease in the overpotential for biomolecules, and enhance the electrochemical signal. RTILs have been used as the modifier for the fabrication of different kinds of chemically modified electrode for the detection of low molecular weight substances such as nitric oxide, dopamine, and ascorbic acid [30–32]. The direct electrochemistry of a redox protein has also been investigated in an RTIL chemically modified electrode [31].

In the present work, a novel architecture was designed by combining good electrochemical performance of RTILs, the redox electrochemistry of PB, and excellent adsorption of AuNPs to HIgG. A room temperature ionic liquid, 1-octyl-3-methylimidazolium hexafluorophosphate ($OMIMPF_6$), was used in the preparation of the carbon ionic liquid electrode to accelerate the rate of electron transfer of the immunosensor. The PB film was electrodeposited on the surface of the CILE, and APS was then coated on the surface of the PB film to form a stable film with excellent redox activity and good biocompatibility. Subsequently, AuNPs were adsorbed onto the APS/PB composite surface through the well-known interaction between AuNPs and amino groups of APS, which provided an interface for immobilization of HIgG. After the assembly of HIgG, bovine serum albumin (BSA) was employed to block any remaining active sites of the AuNPs layer to prevent nonspecific binding. The results showed that this immobilization technique was effective in preventing the leakage of both mediator and antibodies. The presence of AuNPs not only allowed firm attachment of HIgG under mild, physiological conditions, but also enhanced the conductivity of the resulting film. Compared with conventional immunoassay methods, the developed immunosensor was simple, economical, and efficient in the quantification of HIgG.

Experimental

Materials

Chloroauric acid and graphite powder (extra pure) were obtained from Shanghai Reagent Company (Shanghai, China). 3-Aminopropyl triethylene silane (APS) was obtained from Shuguang Chemical Co. (Nanjing, China). Bovine serum albumin (BSA), human serum albumin (HSA), goat anti-human IgG monoclonal antibody (anti-HIgG), human IgG (HIgG), alpha-fetoprotein, carcinoembryonic antigen, low density lipoprotein, L-cysteine, L-glutamate, L-lysine, ascorbic acid, and dopamine were obtained from Sigma (St.

Louis, MO, USA). 1-Octyl-3-methylimidazolium hexafluorophosphate ($OMIMPF_6$) was obtained from Chengjie Chemical Co., Ltd (Shanghai, China). All other reagents were of analytical grade. Doubly distilled water was used throughout.

Instruments

A CHI660A electrochemical workstation (CH Instruments, USA) and a standard three-electrode cell containing a platinum wire auxiliary electrode, a saturated calomel reference electrode (SCE), and the modified electrode as working electrode were employed for electrochemical studies. All potential values given below refer to SCE.

Preparation of gold nanoparticles

Au nanoparticles were prepared by a method previously reported [33] with a slight modification. Thus, 200 mL of water and 2 mL of 1% (w/w) $HAuCl_4$ solution were mixed and heated to boiling with continuous stirring. Then 4.0 mL of a 1% (w/w) sodium citrate solution was quickly added. The solution turned purple within 20 s and then wine-red color 60 s later. After 15 min, the heater was removed and the mixture was stirred continuously until cooled. Colloidal Au solution was obtained and stored in a dark glass bottle at 4 °C before use.

Construction of CILE

The CILE was fabricated as follows: graphite powder and $OMIMPF_6$ (4:1, w/w) were mixed in a mortar until a homogeneous paste was obtained. The prepared carbon paste was tightly packed into a PVC tube (internal diameter 3 mm) and a cope wire was introduced into the other end for electrical contact. Prior to use, the surface of the electrode was smoothed with a weighing paper.

Fabrication of the immunosensor

An aqueous solution containing 2 mM $FeCl_3$, 2 mM $K_3[Fe(CN)_6]$, 0.1 M KCl, and 0.1 M HCl was deaerated by purging with argon for 10 min. Then PB was deposited on the CILE by applying a constant potential of +0.4 V (vs. SCE) for 120 s. After carefully washing with water, the electrode was transferred into the supporting electrolyte solution consisting of 0.1 M KCl and 0.1 M HCl, and was cycled 20 times between −0.05 and +0.35 V at a scan rate of 50 mV s^{-1}. The redox peak current increased with the number of voltammetric scans, indicating that an electroconductive film formed on the electrode surface. The surface coverage of PB on the modified electrode was estimated from the cyclic voltammogram using the following equation: $\Gamma_c = Q/(nFA)$, where Q is the charge in coulombs, n is the number of electrons involved in the process, F is the Faraday constant, and A is the geometric area of the working electrode in square centimeters. The calculated surface concentration of PB was 3.2×10^{-8} mol cm^{-2}. The resultant PB film modified electrode (PB/CILE) was washed with water and dried with nitrogen. Subsequently, the cleaned PB/CILE was immersed in APS solution (2%, v/v) for 0.5 h to introduce the amine functional groups and protect the PB film. Then, the electrode was rinsed thoroughly with water and dipped into AuNPs solution for 12 h, then rinsed with water. The immobilization of anti-HIgG to AuNPs was accomplished by immersing the resultant electrode in anti-HIgG solution at 4 °C for 12 h, and then the antibody-modified electrode was thoroughly washed with phosphate buffered saline (PBS). The surface concentration of anti-HIgG on the modified electrode was calculated as 4.6×10^{-10} mol cm^{-2}. Finally the resulting electrode was incubated in BSA solution (0.25%, w/w) for 1 h in order to block any remaining active sites and avoid nonspecific adsorption. After the modified electrode was washed carefully with PBS, the immunosensor was thus fabricated and stored at 4 °C when not in use. A schematic illustration of the immunosensor preparation process is shown in Scheme S1 in the "Electronic supplementary material".

Immunoassay protocol

The prepared immunosensor was incubated in various concentrations of HIgG solution at 37 °C for 20 min. After washing carefully with PBS to remove the nonchemisorbed HIgG, differential pulse voltammetric (DPV) responses of the immunosensor were recorded in 0.1 M PBS (pH 7.0) containing 0.1 M KCl. After the antigen–antibody reaction, the response current of the redox probe PB decreased due to the formation of immunocomplex and was directly proportional to the concentration of antigen. According to this linear relationship, the detection of HIgG in the sample solution could be assessed quantitatively.

Results and discussion

Electrochemistry of the immunosensor

The surface properties of the modified electrode at each step were characterized electrochemically and the results are shown in Fig. 1. The cyclic voltammogram of the CILE showed a relatively flat curve of charging current (Fig. 1a). However, as shown in the inset of Fig. 1, the charging current of the CILE was obviously bigger than that at the carbon paste electrode which was made of graphite powder and paraffin oil (CPE). These findings were closely related

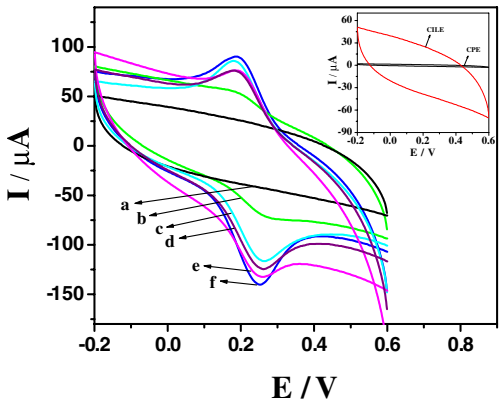

Fig. 1 Cyclic voltammograms of different modified electrodes in pH 7.0 PBS containing 0.1 M KCl at a scan rate of 50 mV s^{-1}. *a* CILE, *b* HIgG/BSA–anti-HIgG/AuNPs/APS/PB/CILE, *c* BSA–anti-HIgG/AuNPs/APS/PB/CILE, *d* anti-HIgG/AuNPs/APS/PB/CILE, *e* APS/PB/CILE, and *f* AuNPs/APS/PB/CILE

to the replacement of nonconductive organic binder with the conductive ionic liquid (IL). On one hand, the IL had large quantities of 'caves' within its molecule structure which made it facile to hold more charges [34]. On the other hand, its good conductive performance facilitated fast transportation and thus reduced surface diffusion capacitance. Therefore, the IL played an important role in promoting the electrochemical performance of the CILE. Furthermore, when PB was electrodeposited on the surface of the CILE and APS was coated on the surface of the electrodeposited PB film, the modified electrode showed a couple of well-defined peaks of PB at 195 and 251 mV (ΔE_p=56 mV, $i_{pc}/i_{pa}\approx 1$) (Fig. 1e), indicating that PB was electrodeposited on the CILE. Deposition of AuNPs increased the conductivity of the APS/PB film, resulting in the increase of the anodic peak and cathodic peak currents (Fig. 1f) as AuNPs act as a conducting wire or an electron communication relay, which increased the electron-transfer efficiency [35]. When the modified electrode was incubated with anti-HIgG, the redox peak currents decreased significantly (Fig. 1d), because the immobilized protein acted as insulator blocking the electron communication of the PB with the electrode. Peak current decreased in the same way after BSA was used to block nonspecific sites (Fig. 1c). After HIgG molecules specifically interacted with the immobilized antibody, the redox peak currents of the PB decreased further (Fig. 1b), indicating the formed immunocomplex might further hinder the electron-transfer pathway of the PB. In addition, the cyclic voltammograms of the immunosensor after being incubated with HIgG were extremely stable during continuous potential cycling between −0.2 and 0.6 V for 0.5 h. These results indicated that the constructed composite biofilm could efficiently prevent leakage of anti-HIgG and retain its high bioactivity.

Figure 2 shows the CVs of the immunosensor in PBS (pH 7.0) at different scan rates. The results demonstrated that both anodic and cathodic peak currents increased linearly with the square root of scan rate between 50 and 800 mV s^{-1} (inset of Fig. 2), suggesting a diffusion-controlled redox process.

Electrochemical impedance spectroscopy (EIS) provides detailed information on the change of the surface properties of modified electrodes for each modification process. Figure 3 shows the impedance spectra corresponding to the stepwise modification processes. The EIS of the CILE (Fig. 3b), APS/PB/CILE (Fig. 3c), and AuNPs/APS/PB/CILE (Fig. 3a) displayed an almost straight line in the Nyquist plot of impedance spectroscopy, characteristic of a diffusion-limited electron-transfer process. In particular, the electron-transfer resistance (R_{et}) of the AuNPs/APS/PB film was the lowest, indicating that AuNPs acted as a good electron relay for shuttling electrons between the electrochemical probe and the electrode. After immobilization of anti-HIgG, an obvious semicircular part of the impedance spectrum appeared, and the R_{et} increased to 533 Ω (Fig. 3d), suggesting that the antibody formed an additional barrier and further prevented electron transfer between the redox probe and the electrode surface. After the electrode was blocked with BSA, the R_{et} increased to 745 Ω (Fig. 3e). This increase was attributed to the fact that the outer protein membrane insulates the conductive support and counteracts the interfacial electron transfer. After immobilization of HIgG onto the electrode surface, a remarkable increase of R_{et} (1,688 Ω) was observed (Fig. 3f). The reason was that the immunocomplex layer on the electrode acted as the electron communication and mass-transfer blocking layer, further insulating the conductive support and hindering the access of the redox probe to the electrode surface significantly. The EIS change of the modified process indicated that the HIgG was immobilized on the modified electrode surface firmly and retained high bioactivity.

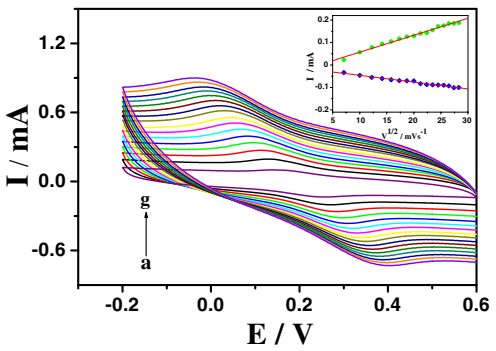

Fig. 2 CVs of the immunosensor in pH 7.0 PBS containing 0.1 M KCl at different scan rates of (from *inner* to *outer*): 50, 100, 150, 200, 250, 300, 350, 400, 450, 500, 550, 600, 650, 700, 750, and 800 mV s^{-1}. The *inset* shows the linear relationship between the peak currents and the square root of scan rate

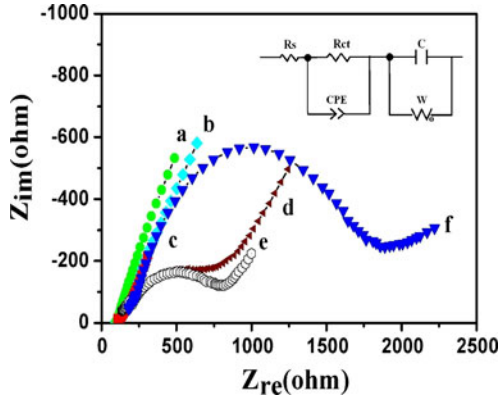

Fig. 3 Nyquist plots of the different electrodes in a PBS (pH 7.0) solution containing 0.1 M KCl and 5.0 mM $Fe(CN)_6^{4-/3-}$: *a* AuNPs/APS/PB/CILE, *b* CILE, *c* APS/PB/CILE, *d* HIgG/AuNPs/APS/PB/CILE, *e* BSA–anti-HIgG/AuNPs/APS/PB/CILE, and *f* HIgG/BSA–anti-HIgG/AuNPs/APS/PB/CILE. The frequency range was from 0.1 to 100,000 Hz with perturbation amplitude of 5 mV. *Inset* equivalent circuit for fitting the plots. *Rs* solution resistance; *Rct* charge-transfer resistance; *CPE* constant phase element, which is a complex of various elements; *C* double-layer capacitance; *W* Warburg resistance, which reflects diffusion barrier in the low frequency part

Also, the depressed arcs in the mid–high frequency section presented typical constant phase element (CPE) characteristics, and they could be fitted by using an RctCPE circuit. The approximately linear curves in the low frequency section were related to capacitance and diffusion resistance, and thus could be fitted by using a CW circuit, in which Warburg impedance (*W*) corresponded to diffusion behavior. An equivalent circuit is showed in Fig. 3 (inset). The result showed that the fitted plots agreed quite well with the measured plots.

Optimum conditions for preparation of CILE

The effect of the mass percent of ion liquid in the mixture (graphite powder and ionic liquid) was investigated in the range of 10–60%. When the mass percent of $OMIMPF_6$ was below 10%, the graphite powder could not be mixed satisfactorily and the mixture was easy to desquamate from the surface of electrode. However, if too much $OMIMPF_6$ was used (i.e., >50%), the mechanical strength of the carbon paste would be too weak and the carbon paste was difficult to shape. As shown in Fig. 4, when the mass percent of $OMIMPF_6$ was 20%, the CV of APS/PB/CILE in PBS exhibited a good shape and the highest peak current. Thus 20% was used in subsequent work.

Optimization of immunoassay procedure

The incubation time of the antigen–antibody reaction in the immunoassay influences the performance of the biosensor. The effect of the incubation time was studied in the range

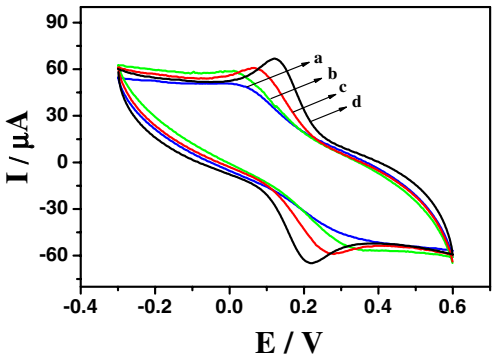

Fig. 4 The effect of mass percent of $OMIMPF_6$. *a* 50%, *b* 40%, *c* 30%, *d* 20%

of 0–40 min. As shown in Fig. 5a, with increasing incubation time, the peak current rapidly decreased and after 20 min the current reached a steady state, indicating the antigen molecules in the solution were completely captured by the immobilized antibody molecules. Therefore, an incubation time of 20 min was used in subsequent work.

The environment temperature also has crucial effect on the activity of the antibody and antigen molecules. The effect of the temperature on the current response of the immunosensor was measured between 20 and 50 °C, and the results are shown in Fig. 5b. Peak current decreased with increasing temperature, and reached a minimum value at 40 °C. When the temperature was increased further, the peak current remained almost unchanged. For practical purposes, the normal body temperature of 37 °C was chosen for all measurements performed with the immunosensor.

Performance of the immunosensor

Under the optimized experimental conditions, the developed immunosensor was exposed to various concentrations of HIgG. After the antigen reacted with the antibody, a DPV curve was collected. As expected, the current response signal decreased with increasing HIgG concentration. This could be rationalized in that more HIgG could bind to the immobilized antibodies at higher concentrations of antigens, and the antigen–antibody complex acted as an inert kinetic barrier to electron transfer by the PB mediator. As a result, the amperometric response decreased with increasing HIgG concentration. As shown in Fig. 6, the decrease of DPV peak current was proportional to the HIgG concentration in two ranges. In the range of 0.05–1.25 ng mL^{-1}, the regression equation was $\Delta I = 2.362C + 2.436$ (ΔI is the change in current response signal before and after the antigen–antibody reactions), and the correlation coefficient was 0.995, with a detection limit of 0.01 ng mL^{-1} at a signal-to-noise (S/N) ratio of 3. In the

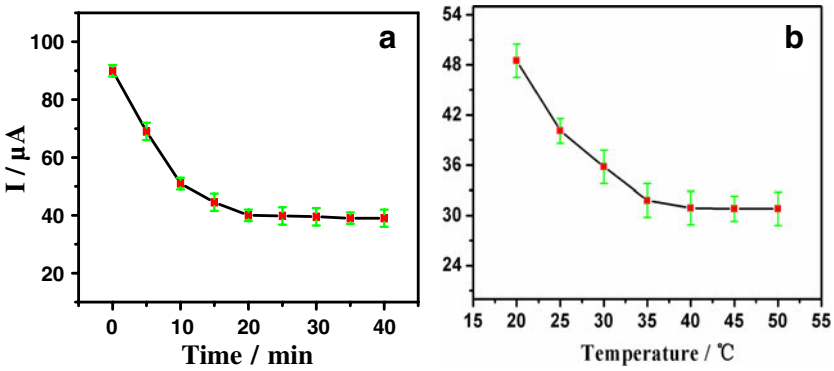

Fig. 5 Effect of incubation time on the amperometric responses of the resulting immunosensor (**a**), and incubation temperature on the amperometric responses of the resulting immunosensor at an incubation temperature of 37 °C (**b**)

range of 1.25–40 ng mL^{-1}, the regression equation was $\Delta I = 0.096C + 4.745$ with a correlation coefficient of 0.993.

The analytical performance of the proposed immunoassay was compared with other electrochemical assays for HIgG determination (Table 1) and suggested the superiority of the present sensor over some earlier reported methods, especially in terms of the detection limit (LOD).

Selectivity of the immunosensor

The specificity of the immunosensor plays an important role in analyzing biological samples in situ without separation since the nonspecific absorption of protein in real matrices influences the performance of a sensing interface. To further characterize the specificity of the immunosensor, the immunosensor was separately incubated in 20 ng mL^{-1} HIgG, 40 ng mL^{-1} alpha-fetoprotein, 40 ng mL^{-1} carcinoembryonic antigen, 40 ng mL^{-1} low density lipoprotein, 40 ng mL^{-1} BSA, 40 ng mL^{-1} HSA, 40 ng mL^{-1} L-cysteine, 40 ng mL^{-1} L-glutamate, 40 ng mL^{-1} L-lysine, 40 ng mL^{-1} ascorbic acid, and 40 ng mL^{-1} dopamine and then detected with the proposed method. The interferential degree of the substance was determined from the value of the current ratio, which was equal to the current value of the immunosensor in the incubation solution containing HIgG and interfering substance versus that only containing HIgG. The results showed that (see Table S1 in the "Electronic supplementary material") the interferents would not cause observable interference to the determination of HIgG, which was attributed to the highly specific antigen–antibody immunoreactions. Furthermore, cross selectivity was also evaluated. When these possible interfering substances simultaneously existed in the incubation solution, the relative standard deviation (RSD) was 4.2% (six measurements), which demonstrated a good selectivity of the immunoassay.

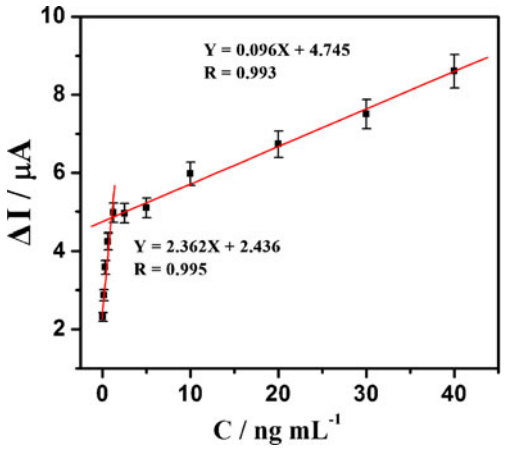

Fig. 6 Calibration curve of the immunosensor for HIgG determination

Reproducibility, stability, and regeneration of the immunosensor

The reproducibility of the proposed immunosensor was evaluated by analyzing HIgG level for six replicate measurements with the proposed method. The RSD was 4.2% at an HIgG concentration of 10 ng mL^{-1}. The fabrication reproducibility of the immunosensor was also evaluated from the amperometric response to 10 ng mL^{-1} HIgG using five different immunosensors made with the same electrode. An RSD of 5.6% was obtained, indicating good reproducibility of the fabrication protocol. The above experimental results indicated the acceptable reproducibility of the proposed immunosensor.

The long-term stability of the immunosensor was also studied over a 30-day period. At different storage periods between 0 and 30 days, the immunosensor was used to detect the same HIgG concentration. As shown in Fig. S1 in the "Electronic supplementary material", the analytical performances did not show an obvious decline and it retained 92% of its initial amperometric value, indicating that the immunosensor had good stability.

Table 1 The performances of the difference modified electrodes for HIgG determination

Modified electrode	Linear range ($ngmL^{-1}$)	LOD ($ngmL^{-1}$)	Stability[a] (percentage/days)	Ref.
Carbon paste electrodes (based on the precipitation of copper on gold nanoparticle tags and subsequent electrochemical stripping detection of the dissolved copper)	2–250	0.5	Not reported	[36]
ZnO/chitosan composite modified GCE	2.5–500	1.2	Not reported	[37]
ITO electrode (anti-IgG labels with horseradish peroxidase doped nanosilica particles (HRP–SiO_2))	1.5–2,250	0.75	89.1%/32	[38]
Carbon paste electrodes (colloidal gold as electrochemical label)	10–500	4	Not reported	[39]
Poly(*o*-phenylenediamine)/AuNPs modified gold electrode	0.025–1	0.01	Not reported	[40]
AuNPs/L-cysteine modified gold disk electrode	0.82–90	0.25	90%/20	[41]
Gold disk electrode (multistep amplification with colloidal gold)	0.015–3.28	0.004	Not reported	[35]
Carbon paste electrodes (based on enzymatic silver deposition on agarose beads)	1–1,000	0.5	Not reported	[42]
Au nano-prickle clusters modified GCE	1–10,000	0.5	Not reported	[43]
Gold colloid modified chitosan nanoparticles-entrapped carbon paste electrode	0.05–1.25 1.25–40	0.01	92%/30	This work

GCE glassy carbon electrode

[a] The biosensor stability is reported as the percentage of its initial response retained after the storage period shown

Regeneration is a key factor in the application and development of immunosensors. The immunosensor can be regenerated by breaking of antigen–antibody bonds. In this work, the regeneration of the immunosensor was achieved by simply immersing it in 0.2 mol L^{-1} glycine hydrochloric acid buffer solution (pH 2.8) for about 6 min followed by washing with PBS several times to desorb the binding antigens. The immunosensor was then incubated in 20 ng mL^{-1} HIgG. Consecutive measurements were repeated for five times and the test results are shown in Table S2 in the "Electronic supplementary material". The RSD of renewable electrodes for HIgG determination was 4.1%.

Application of the immunosensor

In order to evaluate the feasibility of the proposed method for possible applications, the immunosensor was applied to the determination of five different concentrations of HIgG by standard addition methods in three human serum samples. As shown in Table S3 in the "Electronic supplementary material", the recoveries were in the range of 95.6–106.0%, which indicated that the developed immunoassay might be preliminarily applied for the determination of HIgG for routine clinical diagnosis.

Furthermore, the feasibility and the accuracy of HIgG determination was also evaluated by comparing the results obtained from several real samples with the proposed immunoassay system and ELISA, which was a useful and powerful method for serum samples analysis. Table 2 describes the correlation between the results obtained by the proposed immunosensor and the ELISA method. Both results were clearly in acceptable agreement. Therefore, the developed immunoassay methodology could be potentially useful for determination of HIgG in biological samples.

Conclusions

This work described a novel strategy for developing an amperometric immunosensor for HIgG based on a multi-layer biofilm modified carbon ionic liquid electrode. The developed method offers several attractive features: First, ionic liquid $OMIMPF_6$ provided a remarkable increase in the electron-transfer rate of PB and obviously enhanced the electrochemical signal. Second, the APS film not only prevented the leakage of PB from the matrix, but also showed excellent biocompatibility. In particular, with the fixed PB molecules on the electrode surface, no labeling

Table 2 Comparison of HIgG levels determined by using the proposed method and ELISA

Serum samples	1	2	3	4	5
Immunosensor ($ng\ mL^{-1}$)[a]	0.21	0.87	16.32	46.47	94.48
ELISA ($ng\ mL^{-1}$)[a]	0.20	0.82	15.37	49.86	101.81
Relative deviation (%)	5.0	6.1	6.2	−6.8	−7.2

[a] The average value of six successive determinations

molecules were needed in the electrolytical solution, which might greatly simplify the immunoassay process. Finally, based on APS/PB redox film, further chemisorbed AuNPs presented an excellent environmental and electrochemical stability, which could absorb the HIgG under mild, physiological conditions without the loss of their biological activities. Therefore, the biosensor exhibited high response sensitivity, low detection limit, and wide linear range to HIgG. Although only a single antibody/antigen pair (anti-HIgG and HIgG) was illustrated in this strategy, it is expected that the application of this general method to other antibodies should yield immunosensors for the detection of other antigens or compounds of biological importance.

Acknowledgments This work was supported by National Natural Science Foundation of China (20805040, 20635020), Excellent Youth Foundation of He'nan Scientific Committee (104100510020), China Postdoctoral Science Foundation funded project (200902508, 20080430163), Jiangsu Planned Projects for Postdoctoral Research Funds (0801041B), and sponsored by Program for Science & Technology Innovation Talents in Universities of Henan Province (2010HASTIT025).

References

1. Duffy MJ, Van Dalen A, Haglund C, Hansson L, Klapdor R, Lamerz R, Nilsson O, Sturgeon C, Topolcan O (2003) Clinical utility of biochemical markers in colorectal cancer: European Group on Tumour Markers (EGTM) guidelines. Eur J Cancer 39:718–727
2. Hernadez L, Espasa A, Fenandez C, Candela V, Martin C, Romero S (2000) CEA and CA 549 in serum and pleural fluid of patients with pleural effusion. Lung Cancer 36:83–89
3. Morozov VN, Morozova TY (2003) Electrophoresis-assisted active immunoassay. Anal Chem 75:6813–6819
4. Ehrhart J, Bennetau B, Renaud L, Madrange J, Thomas L, Morisot J, Brosseau A, Tran P (2008) A new immunosensor for breast cancer cell detection using antibody-coated long alkylsilane self-assembled monolayers in a parallel plate flow chamber. Biosens Bioelectron 24:467–474
5. Kim N, Kim D, Cho Y, Moon D, Kim W (2008) Carp vitellogenin detection by an optical waveguide lightmode spectroscopy biosensor. Biosens Bioelectron 24:391–396
6. Wasowicz M, Viswanathan S, Dvornyk A, Grzelak K, Kludkiewicz B, Radecka H (2008) Development of an oligo(ethylene glycol)-based SPR immunosensor for TNT detection. Biosens Bioelectron 24:191–197
7. Yang Z, Fu Z, Yan F, Liu H, Ju H (2008) A chemiluminescent immunosensor based on antibody immobilized carboxylic resin beads coupled with micro-bubble accelerated immunoreaction for fast flow-injection immunoassay. Biosens Bioelectron 24:35–40
8. Campas M, Marty J (2007) Enzyme sensor for the electrochemical detection of the marine toxin okadaic acid. Anal Chim Acta 605:87–93
9. Pohanka M, Skladal P (2008) Electrochemical biosensors - principles and applications. J Appl Biomed 6:57–64
10. Li J, Tan SN, Ge H (1996) Silica sol-gel immobilized amperometric biosensor for hydrogen peroxide. Anal Chim Acta 335:137–138
11. Razumiene J, Meškys R, Gurevièiene V, Laurinavièius V, Reshetova MD, Ryabov AD (2000) 4-Ferrocenylphenol as an electron transfer mediator in PQQ-dependent alcohol and glucose dehydrogenase-catalyzed reactions. Electrochem Commun 2:307–311
12. Yu H, Yan F, Dai Z, Ju H (2004) A disposable amperometric immunosensor for α-1-fetoprotein based on enzyme-labeled antibody/chitosan-membrane-modified screen-printed carbon electrode. Anal Biochem 331:98–105
13. Lei CX, Wu J, Wang H, Shen GL, Yu RQ (2004) A new electrochemical immunoassay strategy for detection of transferrin based on electrostatic interaction of natural polymers. Talanta 63:469–474
14. Li N, Yuan R, Chai Y, Chen S, An H, Li W (2007) New antibody immobilization strategy based on gold nanoparticles and Azure I/multi-walled carbon nanotube composite membranes for an amperometric enzyme immunosensor. J Phys Chem C 111:8443–8450
15. Fiorito PA, Goncales VR, Ponzio EA (2005) Synthesis, characterization and immobilization of Prussian blue nanoparticles: a potential tool for biosensing devices. Chem Commun 5:366–368
16. Oliveira MF, Mortimer RJ, Stradiotto NR (2000) Voltammetric determination of persulfate anions using an electrode modified with a Prussian blue film. Microchem J 64:155–160
17. Ricci F, Moscone D, Tuta CS, Palleschi G, Amine A, Poscia A, Valgimigli F, Messeri D (2005) Novel planar glucose biosensors for continuous monitoring use. Biosens Bioelectron 20:1993–2000
18. Zhao G, Feng JJ, Zhang QL, Li SP, Chen HY (2005) Synthesis and characterization of Prussian blue modified magnetite nanoparticles and its application to the electrocatalytic reduction of H_2O_2. Chem Mater 17:3154–3159
19. Zhou P, Xue D, Luo H, Chen X (2002) Structure and magnetic properties of highly ordered Prussian blue nanowire arrays. Nano Lett 2:845–847
20. Mattos IL, Lukachova LV, Gorton L, Laurell T, Karyakin AA (2001) Evaluation of glucose biosensors based on Prussian Blue and lyophilised, crystalline and cross-linked glucose oxidases (CLEC®). Talanta 54:963–974
21. Karyakin AA, Puganova EA, Budashov IA, Kurochkin IN, Karyakina EE, Levchenko VA, Matveyenko VN, Varfolomeyev SD (2004) Prussian blue based nanoelectrode arrays for H_2O_2 detection. Anal Chem 76:474–478
22. Garjonyte R, Malinauskas A (1999) Operational stability of amperometric hydrogen peroxide sensors, based on ferrous and copper hexacyanoferrates. Sens Actuators B 56:93–97
23. Liu ZM, Yang Y, Wang H, Liu YL, Shen GL, Yu RQ (2005) A hydrogen peroxide biosensor based on nano-Au/PAMAM dendrimer/cystamine modified gold electrode. Sens Actuators B 106:394–400
24. Xiao Y, Patolsky F, Katz E, Hainfeld JF, Willner I (2003) "Plugging into enzymes": nanowiring of redox enzymes by a gold nanoparticle. Science 299:1877–1881
25. Parak WJ, Pellegrino T, Micheel CM, Gerion D, Williams SC, Alivisatos AP (2003) Conformation of oligonucleotides attached to gold nanocrystals probed by gel-electrophoresis. Nano Lett 3:33–36
26. Gole A, Dash C, Soman C, Sainkar SR, Rao M, Sastry M (2001) On the preparation, characterization, and enzymatic activity of fungal protease-gold colloid bioconjugates. Bioconjug Chem 12:684–690
27. Chen SH, Yuan R, Chai YQ, Xu Y, Min LG, Li N (2008) A new antibody immobilization technique based on organic polymers protected Prussian blue nanoparticles and gold colloidal nanoparticles for amperometric immunosensors. Sens Actuators B 135:236–244
28. Abbaspour A, Mehrgardi MA (2004) Electrocatalytic oxidation of guanine and DNA on a carbon paste electrode modified by cobalt hexacyanoferrate films. Anal Chem 76:5690–5696
29. Lawrence NS, Deo RP, Wang J (2004) Biocatalytic carbon paste sensors based on a mediator pasting liquid. Anal Chem 76:3735–3739

30. Li CM, Zang JF, Zhan DP, Chen W, Sun CQ, Teo AL, Chua YT, Lee VS, Moochhala SM (2006) Electrochemical detection of nitric oxide on a SWCNT/RTIL composite gel microelectrode. Electroanalysis 18:713–718
31. Sun W, Yang MX, Gao RF, Jiao K (2007) Electrochemical determination of ascorbic acid in room temperature ionic liquid Bpp f6 modified carbon paste electrode. Electroanalysis 19:1597–1602
32. Yan QP, Zhao FQ, Li GZ, Zeng BZ (2006) Voltammetric determination of uric acid with a glassy carbon electrode coated by paste of multiwalled carbon nanotubes and ionic liquid. Electroanalysis 18:1075–1080
33. Frens G (1973) Controlled nucleation for the regulation of the particle size in monodisperse gold suspensions. Nat Phys Sci 241:20–22
34. Yoshio M, Mukai T, Ohno H, Kato T (2004) One-dimensional ion transport in self-organized columnar ionic liquids. J Am Chem Soc 126:994–995
35. Chen H, Jiang JH, Huang Y, Deng T, Li JS, Shen GL, Yu RQ (2006) An electrochemical impedance immunosensor with signal amplification based on Au-colloid labeled antibody complex. Sens Actuators B 117:211–218
36. Mao X, Jiang JH, Luo Y, Shen GL, Yu RQ (2007) Copper-enhanced gold nanoparticle tags for electrochemical stripping detection of human IgG. Talanta 73:420–424
37. Wang ZJ, Yang YH, Li JS, Gong JL, Shen GL, Yu RQ (2006) Organic–inorganic matrix for electrochemical immunoassay: detection of human IgG based on ZnO/chitosan composite. Talanta 69:686–690
38. Zhong ZY, Li MX, Xiang DB, Dai N, Qing Y, Wang D, Tang DP (2009) Signal amplification of electrochemical immunosensor for the detection of human serum IgG using double-codified nanosilica particles as labels. Biosens Bioelectron 24:2246–2249
39. Chen ZP, Peng ZF, Zhang P, Jin XF, Jiang JH, Zhang XB, Shen GL, Yu RQ (2007) A sensitive immunosensor using colloidal gold as electrochemical label. Talanta 72:1800–1804
40. Zhang SB, Zheng F, Wu ZS, Shen GL, Yu RQ (2008) Highly sensitive electrochemical detection of immunospecies based on combination of Fc label and PPD film/gold nanoparticle amplification. Biosens Bioelectron 24:129–135
41. Zhang LY, Liu Y, Chen T (2008) A mediatorless and label-free amperometric immunosensor for detection of h-IgG. Int J Biol Macromol 43:165–169
42. Luo Y, Mao X, Peng ZF, Jiang JH, Shen GL, Yu RQ (2008) A new strategy for electrochemical immunoassay based on enzymatic silver deposition on agarose beads. Talanta 74:1642–1648
43. Wang SP, Wu ZS, Qu FL, Zhang SB, Shen GL, Yu RQ (2008) A novel electrochemical immunosensor based on ordered Au nanoprickle clusters. Biosens Bioelectron 24:1020–1026